



Article

Automated Multistep Lateral Flow Immunoassay Using a Smartphone for the Quantification of Foodborne Bacteria from Fresh Lettuce

Pattarapon Phangwipas¹, Balamurugan Thangavel¹ and Joong Ho Shin^{1,2,*} ¹ Department of Biomedical Engineering, Pukyong National University, Busan 48513, Republic of Korea² Industry 4.0 Convergence Bionics Engineering, Pukyong National University, Busan 48513, Republic of Korea

* Correspondence: jhshin@pknu.ac.kr

Abstract: Foodborne illnesses are one of the most severe and prevalent health problems in the world. Thus, achieving the rapid and accurate identification of foodborne pathogens is important. This study presents an automatic device to perform a multistep immunoassay on a lateral flow immunoassay strip to detect foodborne pathogens from fresh lettuce. The device is automatically operated using a smartphone application that we developed, which allows users to quantify the detection results. In this study, we characterize the device's limit of detection and demonstrate the detection and quantification of *Escherichia coli* O157:H7 from contaminated lettuce. We then compare the quantified result to that calculated by counting colonies from agar plates. The device is capable of detecting contamination in lettuces that have as low as 5×10^4 *Escherichia coli* O157:H7 per 10 g.

Keywords: contamination; pathogenic bacteria; smartphone; lateral flow immunoassay; automatic detection; immunosensor; *Escherichia coli* O157:H7



Citation: Phangwipas, P.; Thangavel, B.; Shin, J.H. Automated Multistep Lateral Flow Immunoassay Using a Smartphone for the Quantification of Foodborne Bacteria from Fresh Lettuce. *Chemosensors* **2023**, *11*, 36. <https://doi.org/10.3390/chemosensors11010036>

Academic Editor: Jin-Ming Lin

Received: 18 November 2022

Revised: 26 December 2022

Accepted: 28 December 2022

Published: 2 January 2023



Copyright: © 2023 by the authors. Licensee MDPI, Basel, Switzerland. This article is an open access article distributed under the terms and conditions of the Creative Commons Attribution (CC BY) license (<https://creativecommons.org/licenses/by/4.0/>).

1. Introduction

Foodborne illnesses are a major public health problem worldwide and one of the major sources of morbidity and mortality in both developed and developing nations [1]. The World Health Organization (WHO) reports that almost 1 in 10 people in the world fall ill after eating contaminated food, and 420,000 die every year [2,3]. Bacteria, viruses, parasites, or chemical substances enter the body through contaminated food, and they are the leading cause of foodborne illness [4]. One of the most dominant foodborne illnesses are outbreaks from the consumption of fresh fruit and vegetables (fresh produce). This is because the number of people consuming fresh produce has been increasing over the years [5–7]. Thus, there should be a rapid detection method to prevent fresh produce contamination.

The gold standard of traditional techniques for pathogen detection in fresh produce is a culture-based method [8]. The method relies on a series of processes that involve stomaching, enrichment, bacteria culture, and the identification of target bacteria. First, the food sample is placed in a sterile plastic bag with the bacteria growth medium, and then the plastic bag is placed in a stomacher machine to remove the bacteria from the food sample. Then, the extracts are incubated for 18–25 h to enrich and to increase the number of bacteria [9]. The enriched sample is streaked and incubated for an additional 24 h on an agar plate for colony analysis. To ensure purity, the colonies must be isolated and incubated, after which they become visible to the naked eye [10]. However, the culture process typically requires more than 2 days to analyze the results [11].

Many researchers have developed several methods for rapid detection, such as PCR-based methods (polymerase chain reaction (PCR) [12], real-time PCR or quantitative PCR (qPCR) [13], and loop-mediated isothermal amplification (LAMP) [14,15]), owing to the limitations of the culture-based method, such as a long time for analyzing the results. The PCR-based methods are accurate and sensitive; however, they require complicated PCR

mix preparation and bulky instruments such as a thermocycler. As a more convenient alternative, immunological-based methods (immunoassay) are employed. Immunoassays are based on antibody–antigen interactions, in which an antibody is used to bind or to capture target-specific antigens [16]. Among many immunoassays, detection using enzyme-linked immunosorbent assay (ELISA) and lateral flow immunoassay (LFIA) are widely investigated [17]. Several studies report that the detection of the ELISA process was highly accurate and sensitive, with a limit of detection (LOD) of 1×10^4 CFU/mL [18]. However, sophisticated techniques, antibody instability, and the need for expensive culture media and trained technicians hinder its usage [19]. The advantage of LFIA is that it is rapid, simple, cheap, and suitable for on-site detection [16]. However, one of the main disadvantages of LFIA is its relatively high limit of detection. Thus, several methods have been employed to overcome this disadvantage. For example, subsequently adding chemical reagents, such as gold nanoparticle (AuNPs) enhancers to AuNP labels [20] or chemiluminescence substrates to enzyme labels [21], has been proven to effectively improve the sensitivity of the detection. Another way to improve the detection limit is to use a multistep assay such as ELISA. Previous research has shown that ELISA can be performed on LFIA to detect *Escherichia coli* (*E. coli*) O157:H7 [22]. The assay involves capturing and labeling the bacteria, and employing a signal generation step. However, in order to introduce the reagent required for signal generation, a sample pad and an absorbent pad must be manually placed. In order to overcome such a limitation, handheld devices based on rotary-type devices were proposed [10,23]. The devices consist of two layers: a top layer containing multiple sample pads and absorbent pads, and a bottom layer containing a nitrocellulose (NC) test strip. The top layer has holes that connect the two ends of the NC strip to the sample and absorbent pads. When the reagent is loaded into the sample pad, the sample flows through the NC test strip and is then absorbed by the absorbent pad. After a desired duration of sample flow, the device is rotated to align the subsequent pads and to introduce the subsequent reagents. However, the user must manually rotate the device and wait during each reagent step, necessitating the development of an automated detection system.

In this study, we developed a smartphone-operated platform and a smartphone application that can automate bacteria detection and analysis. It consists of a disposable rotary device that can rotate automatically using a servo motor, which is controlled by a smartphone application via Bluetooth. The platform has a cover box that allows for consistent imaging of the signal from the test strip using a phone camera to quantify the bacteria. To quantify the bacteria, the application was used to create a calibration curve and to calculate the unknown signal intensity. Here, we report the device and fabrication, perform multistep immunoassay on LFIA, and demonstrate the simple colorimetric detection of *E. coli* O157:H7.

2. Materials and Methods

2.1. Materials and Reagents

A total of 1 mg/mL of goat anti-rabbit IgG (R5506; Sigma-Aldrich, St. Louis, MO, USA) was dispensed as a control line, and 1 mg/mL of mouse *E. coli* O157 antibody (MBS568193; My BioSource, San Diego, CA, USA) was dispensed as a test line on the NC membrane (NCPF-SN12, mdi Membrane Technologies, Inc., Camp Hill, PA, USA), and allowed to dry at room temperature. Horseradish peroxidase (HRP)-conjugated anti-*E. coli* IgG (ab20425; Abcam, Cambridge, UK) was diluted to 10 ng/mL in phosphate-buffered saline (PBS) containing 3% BSA and 0.05% Tween-20, and used as a labeling agent. PBS containing 3% BSA and 0.05% Tween-20 was used as a wash buffer. The 3,3'-diaminobenzidine (DAB) (Sigma-Aldrich) solution was prepared by dissolving and mixing in 5 mL of deionized water (DI water) using Vortex-Genie 2 (Scientific Industries, Bohemia, NY, USA), and this was used as a substrate. *E. coli* O157:H7 (ATCC 35150) was used as a target bacteria, and *S. aureus* (ATCC 12600), and *S. Typhimurium* (ATCC 14028) were used to observe the detection specificity. For the strip stability test, 1 mg/mL goat anti-rabbit IgG containing

1% trehalose and 1 mg/mL mouse *E. coli* O157 antibody containing 1% trehalose were dispensed onto an NC membrane. The NC membrane with immobilized antibodies were stored at 4 °C in a box to prevent exposure to light.

2.2. Design and Fabrication

This device is divided into two main parts: the operating platform (electronics) and the disposable rotary devices, as shown in Figure 1a. The operating platform was designed using SOLIDWORKS software and printed using the Sindoh 3D Printer (3DWOX 1, Sindoh, Republic of Korea). This part consists of the operating platform box and cover box. The operating platform box contains a Bluetooth (HC-06 Bluetooth Module, P0000PKG; Anyang, Republic of Korea) and servo motor that allows the device to rotate. The cover box prevents variations in ambient light during imaging by providing a dark room for the smartphone. A jig for uniformly positioning the smartphone is included in the cover box. The rotary parts consist of the bottom piece and the top piece (the rotating part), which are made from 3 mm thick poly (methyl methacrylate) (PMMA) plates, and were patterned and etched using a laser cutter (KL-900L; KISON, Seongnam, Republic of Korea).

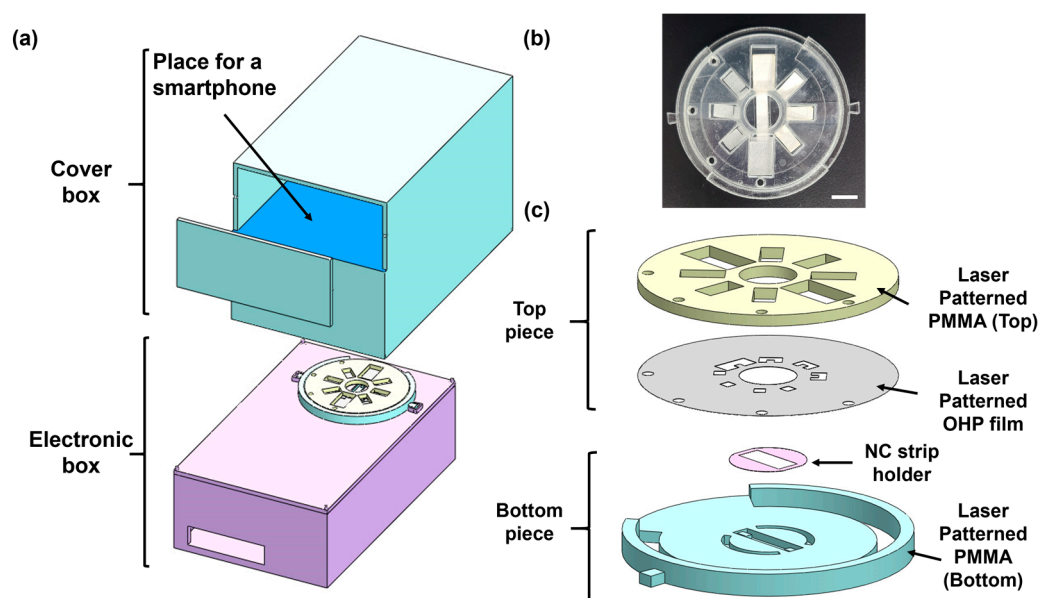


Figure 1. (a) Schematic of the operating platform showing the cover box and the electronic box with the rotary device placed inside. (b) Photo of the rotary device with the NC membrane, glass fiber pads, and absorbent pads installed in it. Scale bar = 1 cm. (c) Exploded view of the rotary device showing each layer and its components.

The diameter of the rotary pad (top piece) was 67 mm, which contains 4 sample pads and 4 absorbent pads (Figure 1b). The through-holes were patterned on the OHP film with a laser cutter and attached to the top piece with double-sided tape. The NC test strip was placed on the center of the bottom piece. The NC strip holder was patterned and cut on the OHP film, and attached to the bottom piece, as shown in Figure 1c. The bottom piece has an arc-shaped cut-out, and the top piece has four circular holes, which are used for fixing the prongs (connected to the servo motor) so that the top piece can be rotated by the servo motor without rotating the bottom piece, which is fixed by the key (Figure S1). The servo motor rotates the top piece, waits for a specified duration for reagent flow, and then rotates again to introduce a subsequent reagent to the NC strip. The series of wait-and-rotate movements allows the user to perform an automated multistep assay on a lateral flow immunoassay (LFIA) strip.

2.3. Application Development

The application was developed using the MIT app inventor and operates by using the Samsung Galaxy S20 +5G (Samsung, Republic of Korea), which consists of 3 functions: Setting and Run, Calibration, and Calculation, as shown in Figure 2a. The first function is Setting and Run, as shown in Figure 2b. On this screen, the user can connect the application to the device via Bluetooth. The assay starts with the user setting the duration for the assay step (this study used 10, 5, 5, and 10 min for the assay step sequence), and the timer begins counting down upon clicking the start button. During the countdown, the reagents are delivered from the sample pad to the absorbent pad via capillary force. The device is automatically rotated 45° counterclockwise to the next step of the assay when the set time or the countdown reaches zero. The second function is Calibration, which is used to make a calibration curve from known bacteria concentrations. In this study, we used the bacteria *E. coli* O157:H7 with a concentration ranging from 5×10^0 to 5×10^7 CFU/mL for performing automated multistep LFIA. After the result, or a signal from the test line, appears on the NC membrane, its image is captured using the smartphone, and the application quantifies the signal intensity, as shown in Figure 2c. Then, the calibration curve will be made based on a regression equation (Figure 2d,e). Lastly, the Calculation (Figure 2f) function calculates the concentration of bacteria in a liquid sample based on the calibration curve. When the signal from the unknown sample, which is the intensity of the signal on the test line of the NC membrane, is quantified and input into the application, the user can calculate an estimated bacterial concentration based on the calibration curve.

2.4. Principle of Performing Automated Multistep LFIA

As shown in Figure 3a, the first sample pad (S1) was designed to contain 90 µL of the sample, and the other sample pads (S2–S4) were designed to contain 40 µL of the assay reagents. The assay commenced by loading 90 µL of *E. coli* O157:H7 suspended in 2% bovine serum albumin (BSA) into S1, then allowing the sample to flow for 10 min. While the sample containing the bacteria is delivered through the NC membrane, the target bacteria is captured by the antibodies immobilized at the test line, as shown in Figure 3b.

Before loading the sample into S1, S2 was loaded with HRP-conjugated anti-*E. coli* IgG, wash buffer was loaded into S3, and DAB solution was loaded into S4. After 10 min of sample flow, the rotary device (top piece) automatically rotates 45° counterclockwise to deliver HRP-conjugated anti-*E. coli* IgG, which was in S2. In this step, the HRP-conjugated IgG binds with the captured bacteria at the test line and anti-rabbit IgG at the control line, as shown in Figure 3c. After 5 min of the IgG flow, the rotary device automatically rotates to deliver the wash buffer for 5 min to eliminate non-specific bacteria from the NC membrane, as shown in Figure 3d. Lastly, after finishing the wash step, the rotary pad rotates again to perform the next step. In the last step, the DAB solution flows through the NC membrane to generate the signal for 10 min. The DAB is oxidized by hydrogen peroxide to change the color to brown, which allows the signal to be shown on the NC membrane, as shown in Figure 3e. The assay can be automatically finished in less than 30 min using the smartphone application and the device.

2.5. Detection of Bacteria from Contaminated Lettuce

E. coli O157:H7 was incubated in a shaking incubator (SHI1; Labtron, Seoul, Republic of Korea) overnight. The optical density (OD) of the bacteria was measured using a spectrophotometer and a growth curve (Figure S2) to quantify the concentration, which was then diluted to 5×10^7 CFU/mL by adding PBS. The solution containing the bacteria was centrifuged at $3000 \times g$ for 20 min, and the bacteria were resuspended in PBS. Then, the bacteria was further diluted to the target concentrations of 5×10^4 , 5×10^5 , and 5×10^6 CFU/mL. In total, 10 µL of each solution containing bacteria were log-diluted and dotted on an agar plate to measure the actual concentration. The colonies on agar plates were counted the next day. A total of 100 µL of each bacteria target was dropped onto the lettuces at different spots and allowed to dry for 5 min before being placed in a plastic bag.

A 45 mL volume of PBS was poured into each plastic bag with lettuce. Then, the bags were shaken for 2–3 min to retrieve the bacteria from the lettuce. The solution from the plastic bag was poured into two 50 mL conical tubes and centrifuged at $3000 \times g$ for 20 min. After removing the supernatants, the samples (the infranatant) were resuspended in 300 μL of PBS in a microcentrifuge tube. A portion of the sample was mixed with BSA to reach the final concentration of 2% BSA. A 90 μL volume of the sample was loaded into the device for detection.

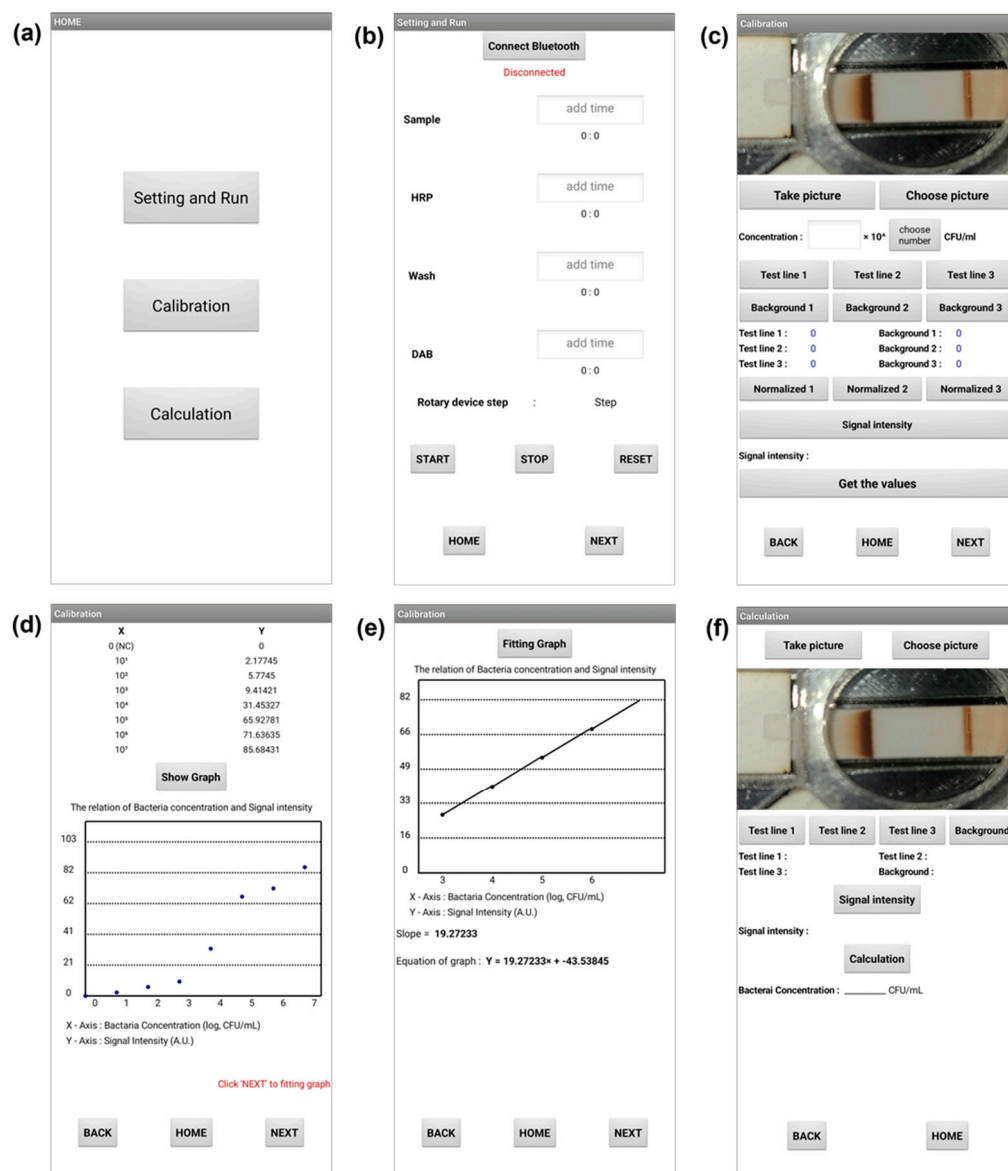


Figure 2. Screenshots of the application for lateral flow immunoassay. (a) First page of the application; the user can select the Setting and Run, Calibration, and Calculation menus. (b) Screen shot of the Setting and Run, which is a page used for inputting flow durations. (c) First page of the Calibration screen, showing the image of the NC strip, and the user can specify the known concentration. (d) Calibration curve. (e) Linear fit curve showing the slope and the equation of the curve. (f) Screen shot of the Calculation, showing the image of the test result of an unknown sample, and the calculated bacteria concentration based on the calibration curve.

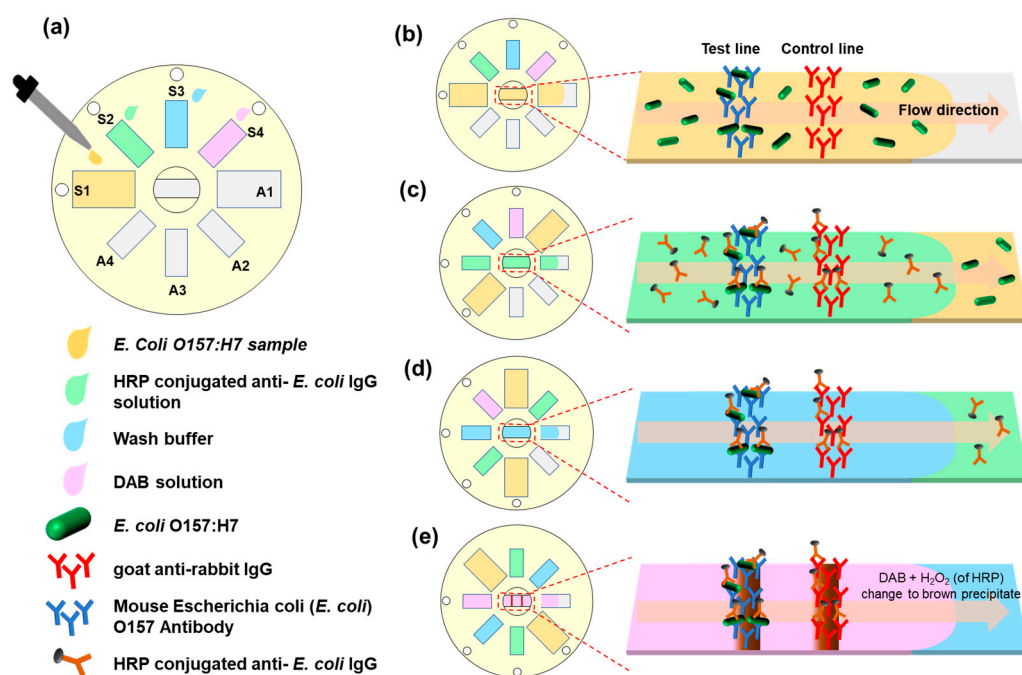


Figure 3. Schematics of each step of strip-based multistep immunoassay showing (a) loading the reagent for assay on the rotary pad, (b) bacteria capture, (c) HRP-IgG labeling, (d) wash, and (e) signal generation using DAB steps.

3. Results and Discussion

3.1. Smartphone Application and Calibration Curve

The *E. coli* O157:H7 samples whose concentrations ranged from 5×10^0 to 5×10^7 CFU/mL were used for making a calibration curve. The signal intensity of each bacterial concentration was calculated from the application. Figure 2d shows the result of the quantified signal intensity with respect to the bacterial concentration, which is used for making the calibration curve. The curve was fit among the data points within the linear range (between 5×10^3 to 10^7 CFU/mL). It is apparent that the signal intensity begins to increase at a bacterial concentration of 5×10^4 CFU (Figure 4a). Thus, based on this result, the LOD of the device by the naked eye is determined to be 5×10^4 CFU/mL. Additionally, by using the phone application and a formula $3.3 \times \text{standard deviation}/\text{slope}$, the LOD is calculated to be $5 \times 10^{1.3}$ CFU/mL (approximately 100 CFU/mL). The calibration curve in Figure 4b was redrawn using OriginLab software to clearly represent the calibration curve made by our application (shown in Figure 2e). The sensitivity of the sensor, or the slope of the linear range (red line) of the calibration curve in Figure 4b, is calculated to be 19.27 intensity (a.u.)/(5×10^1 CFU mL⁻¹). It is important to note that the calibration curve depends on each user and on the experimental condition (i.e., flow duration, antibodies, enzymes, and substrates used); thus, users need to make their own calibration curve before performing target detection in unknown samples.

3.2. Detection Specificity

To observe the specificity of the device, two bacteria of different genera were used, and their detection results were observed (Figure 5a). The result shows a significant difference between the signal intensity when detecting different bacteria of the same concentration (Figure 5b). A faint signal appears when *S. aureus* and *S. Typhimurium* are loaded; however, the intensity is comparable to that of the negative control. This indicates that the detection can be performed with high specificity due to the specificity of the antibody used in this experiment.

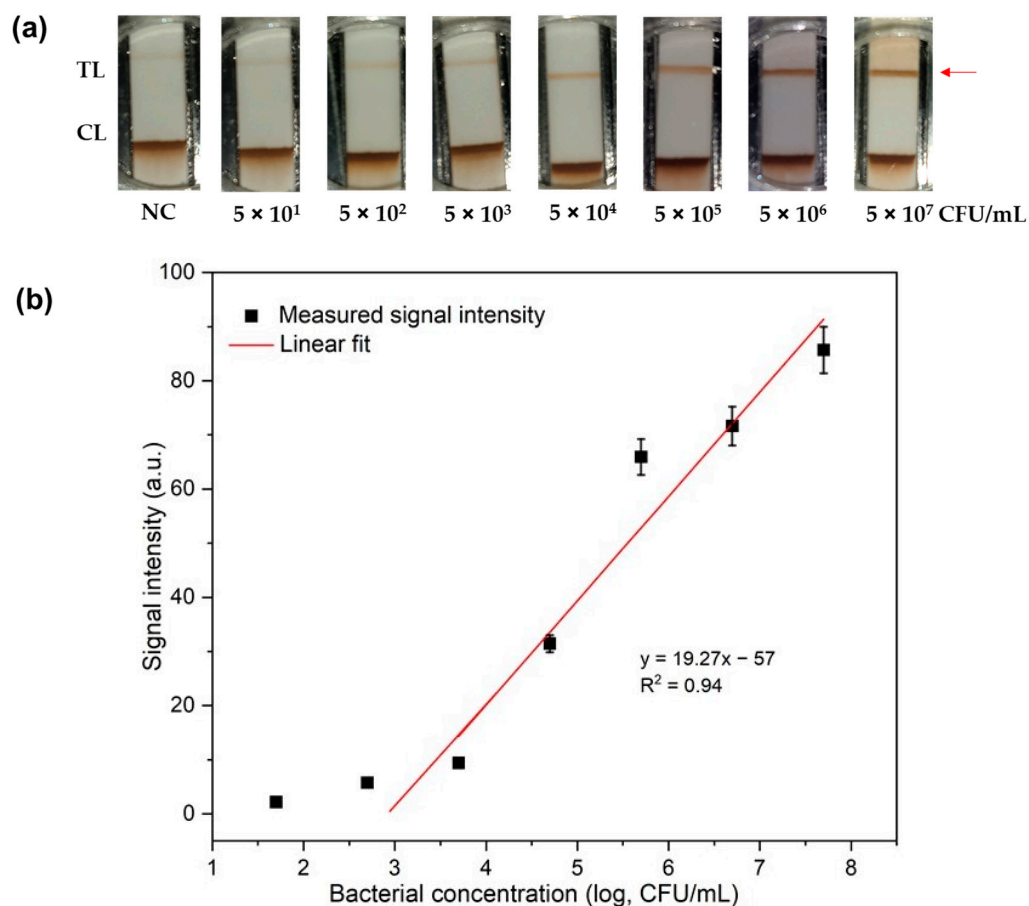


Figure 4. (a) Photos showing the signal generation on the NC strip of bacteria concentration 5×10^0 to 5×10^7 CFU/mL. TL and CL are the test line and control line, respectively. The red arrow indicates the location of the test line. (b) Graph showing the calibration curve and the linear fit.

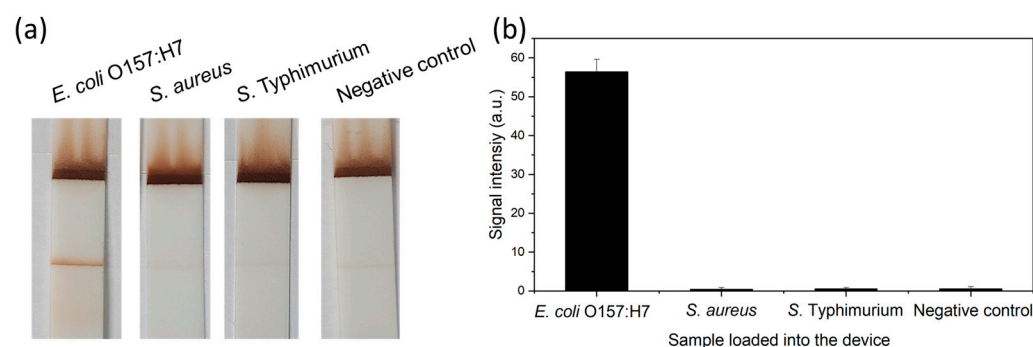


Figure 5. (a) Photos of the detection result of different bacteria. (b) Bar graph of the detection intensities.

3.3. Sensor Stability

The stability of the immobilized antibodies are tested by performing the detection of the same concentration of *E. coli* O157:H7 bacteria (5×10^7 CFU/mL) immediately after immobilizing antibodies onto the NC membrane, and also 5 and 10 days after the immobilization. Figure 6a–c shows photos of the detection result, and shows no apparent difference in the signal intensity. The quantified signal intensity in Figure 6d shows that the error bars of 0, 5, and 10 day storage overlap with each other, which indicates that there is no statistically significant difference between the detection result for at least 10 days.

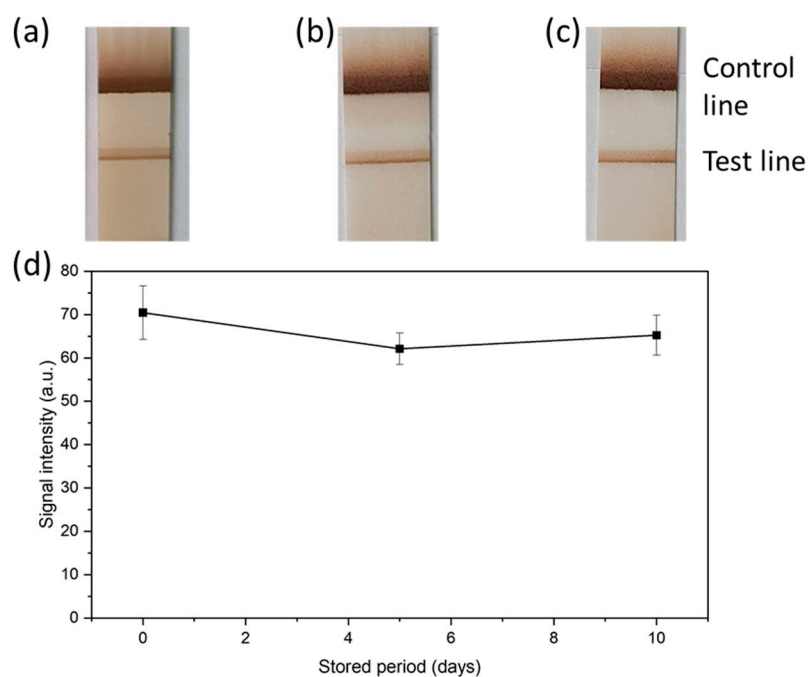


Figure 6. Photos of 5×10^7 CFU/mL *E. coli* O157:H7 (a) immediately after immobilizing antibodies on the NC strip, (b) 5 days after, and (c) 10 days after immobilization. (d) Graph showing the quantified signal intensity of the test line obtained from the stability test.

3.4. Detection of Bacteria from Contaminated Lettuce

The following experiments were performed to validate that the device can detect bacteria from fresh vegetables that are contaminated. In this study, the concentrations of the bacteria target were 5×10^4 , 5×10^5 , and 5×10^6 CFU/mL, based on the linear range (calibration curve) and the limit of detection. The portion of the target bacteria samples prepared for inoculation were dotted on agar and incubated overnight to determine the number of bacteria inoculated into the lettuce. In addition, the bacteria retrieved from the lettuce were diluted and loaded into the device to perform a multistep immunoassay on an LFA strip, and analyzed using the smartphone application. The result (agar and detection signal) of the experiment is shown in Table S1. The calculated concentration obtained from the application was combined with the resuspension volume, inoculation volume, and dilution factor to calculate the number of bacteria retrieved from the lettuce in CFU/10 g (Table 1). There can be some bacteria loss during the retrieval process when collecting bacteria from the contaminated lettuce, which can contribute to the discrepancy between the amounts of inoculated bacteria and the number of the detected bacteria using LFIA. However, the results can be considered to be satisfactory when considering the fact that the order of the measured bacteria number and the order of the calculated bacteria number are the same for all cases.

Table 1. Comparison between the number of bacteria inoculated from counting colonies and the number of bacteria inoculated from the device performing multistep immunoassay on a lateral flow strip.

Trial	Target Samples (CFU/mL)	Number of Bacteria Inoculated to the Lettuce, Calculated via Colony Counting (CFU/10 g)	Number of Bacteria from the Contaminated Lettuce Detected Using LFIA (CFU/10 g)
1	5×10^4	2.37×10^3	3.33×10^3
	5×10^5	2.66×10^4	2.51×10^4
	5×10^6	3.16×10^5	1.85×10^5

Table 1. Cont.

Trial	Target Samples (CFU/mL)	Number of Bacteria Inoculated to the Lettuce, Calculated via Colony Counting (CFU/10 g)	Number of Bacteria from the Contaminated Lettuce Detected Using LFIA (CFU/10 g)
2	5×10^4	1.31×10^3	1.22×10^3
	5×10^5	1.73×10^4	19.8×10^4
	5×10^6	2.13×10^5	2.23×10^5
3	5×10^4	1.85×10^3	1.70×10^3
	5×10^5	2.92×10^4	1.33×10^4
	5×10^6	3.49×10^5	3.43×10^5

4. Conclusions

In this study, we demonstrate an automatic multistep immunoassay platform for detecting bacteria on an LFA strip. A smartphone application was used to control the device via Bluetooth, to perform the experiment. The device also has components to control and to prevent the variation in the ambient light from the external environment when using the smartphone's camera to image the LFA strip. The developed app and device are designed to support the automation of multistep assays requiring multiple pipetting and incubation steps, and to assist untrained personnel in detecting point-of-care needs.

Supplementary Materials: The following supporting information can be downloaded at: <https://www.mdpi.com/article/10.3390/chemosensors11010036/s1>, Figure S1. (a) Photo of the platform without the rotary device. Red arrows show the location of the key slots and prongs. (b) Photo of the platform with the rotary device. The key is placed into the key slot to fix the bottom piece and the prongs penetrate the four holes of the top piece so that the servo motor can rotate the top piece only. Figure S2. Graph showing the relationship between the concentration of bacteria with respect to optical density (at 600 nm). Table S1. Inoculated bacteria on the agar plate for colony counting (only the plates showing 30–300 colonies are chosen for accurate enumeration), and detection signal on the LFA strips.

Author Contributions: Conceptualization, J.H.S.; methodology, P.P. and J.H.S.; software, P.P.; validation, P.P. and J.H.S.; formal analysis, P.P., B.T. and J.H.S.; resources, J.H.S.; data curation, P.P., B.T. and J.H.S.; writing—original draft preparation, P.P. and J.H.S.; writing—review and editing, B.T. and J.H.S.; visualization, P.P., B.T. and J.H.S.; supervision, J.H.S.; project administration, J.H.S.; funding acquisition, J.H.S. All authors have read and agreed to the published version of the manuscript.

Funding: This work was supported by a National Research Foundation of Korea (NRF) grant funded by the Korean government (MSIT) (Nos. 2020R1C1C1003567 and 2022R1A5A8023404).

Institutional Review Board Statement: Not applicable.

Informed Consent Statement: Not applicable.

Data Availability Statement: Not applicable.

Acknowledgments: The authors would like to thank Ye Lin Kim and Thang Tran Huy Le for their contribution in making the growth curve.

Conflicts of Interest: The authors declare no conflict of interest.

References

1. Singha, S.; Thomas, R.; Viswakarma, J.N.; Gupta, V.K. Foodborne illnesses of Escherichia coli O157 origin and its control measures. *J. Food Sci. Technol.* **2022**, 1–10. [\[CrossRef\]](#)
2. Fahey, J.W.; Smilovitz Burak, J.; Evans, D. Sprout microbial safety: A reappraisal after a quarter-century. *Food Front.* **2022**. [\[CrossRef\]](#)
3. WHO. Estimating the Burden of Foodborne Diseases. Available online: <https://www.who.int/activities/estimating-the-burden-of-foodborne-diseases> (accessed on 23 December 2022).

4. WHO. Food Safety. Available online: <https://www.who.int/news-room/fact-sheets/detail/food-safety> (accessed on 26 October 2022).
5. Callejón, R.M.; Rodríguez-Naranjo, M.I.; Ubeda, C.; Hornedo-Ortega, R.; Garcia-Parrilla, M.C.; Troncoso, A.M. Reported foodborne outbreaks due to fresh produce in the United States and European Union: Trends and causes. *Foodborne Pathog. Dis.* **2015**, *12*, 32–38. [[CrossRef](#)] [[PubMed](#)]
6. Carstens, C.K.; Salazar, J.K.; Darkoh, C. Multistate Outbreaks of Foodborne Illness in the United States Associated With Fresh Produce From 2010 to 2017. *Front. Microbiol.* **2019**, *10*, 2667. [[CrossRef](#)]
7. White, A.E.; Tillman, A.R.; Hedberg, C.; Bruce, B.B.; Batz, M.; Seys, S.A.; Dewey-Mattia, D.; Bazaco, M.C.; Walter, E.S. Foodborne Illness Outbreaks Reported to National Surveillance, United States, 2009–2018. *Emerg. Infect. Dis.* **2022**, *28*, 1117–1127. [[CrossRef](#)] [[PubMed](#)]
8. García-Cañas, V.; Simó, C.; Herrero, M.; Ibáñez, E.; Cifuentes, A. Present and future challenges in food analysis: Foodomics. *Anal. Chem.* **2012**, *84*, 10150–10159. [[CrossRef](#)]
9. Priyanka, B.; Patil, R.K.; Dwarakanath, S. A review on detection methods used for foodborne pathogens. *Indian J. Med. Res.* **2016**, *144*, 327–338. [[CrossRef](#)]
10. Shin, J.H.; Hong, J.; Go, H.; Park, J.; Kong, M.; Ryu, S.; Kim, K.P.; Roh, E.; Park, J.K. Multiplexed Detection of Foodborne Pathogens from Contaminated Lettuces Using a Handheld Multistep Lateral Flow Assay Device. *J. Agric. Food Chem.* **2018**, *66*, 290–297. [[CrossRef](#)]
11. Foddai, A.C.G.; Grant, I.R. Methods for detection of viable foodborne pathogens: Current state-of-art and future prospects. *Appl. Microbiol. Biotechnol.* **2020**, *104*, 4281–4288. [[CrossRef](#)]
12. Hill, W.E. The polymerase chain reaction: Applications for the detection of foodborne pathogens. *Crit. Rev. Food Sci. Nutr.* **1996**, *36*, 123–173. [[CrossRef](#)]
13. Strohmeier, O.; Marquart, N.; Mark, D.; Roth, G.; Zengerle, R.; von Stetten, F. Real-time PCR based detection of a panel of food-borne pathogens on a centrifugal microfluidic “LabDisk” with on-disk quality controls and standards for quantification. *Anal. Methods* **2014**, *6*, 2038–2046. [[CrossRef](#)]
14. Lalonde, L.F.; Xie, V.; Oakley, J.R.; Lobanov, V.A. Optimization and validation of a loop-mediated isothermal amplification (LAMP) assay for detection of *Giardia duodenalis* in leafy greens. *Food Waterborne Parasitol.* **2021**, *23*, e00123. [[CrossRef](#)]
15. Lee, J.W.; Nguyen, V.D.; Seo, T.S. Paper-based Molecular Diagnostics for the Amplification and Detection of Pathogenic Bacteria from Human Whole Blood and Milk Without a Sample Preparation Step. *BioChip J.* **2019**, *13*, 243–250. [[CrossRef](#)]
16. Zhao, X.; Lin, C.W.; Wang, J.; Oh, D.H. Advances in rapid detection methods for foodborne pathogens. *J. Microbiol. Biotechnol.* **2014**, *24*, 297–312. [[CrossRef](#)] [[PubMed](#)]
17. Wu, S.-Y.; Hulme, J.; An, S.S.A. Recent trends in the detection of pathogenic *Escherichia coli* O157: H7. *BioChip J.* **2015**, *9*, 173–181. [[CrossRef](#)]
18. Pang, B.; Zhao, C.; Li, L.; Song, X.; Xu, K.; Wang, J.; Liu, Y.; Fu, K.; Bao, H.; Song, D.; et al. Development of a low-cost paper-based ELISA method for rapid *Escherichia coli* O157:H7 detection. *Anal. Biochem.* **2018**, *542*, 58–62. [[CrossRef](#)]
19. Sakamoto, S.; Putalun, W.; Vimolmangkang, S.; Phoolcharoen, W.; Shoyama, Y.; Tanaka, H.; Morimoto, S. Enzyme-linked immunosorbent assay for the quantitative/qualitative analysis of plant secondary metabolites. *J. Nat. Med.* **2018**, *72*, 32–42. [[CrossRef](#)]
20. Pan, R.; Jiang, Y.; Sun, L.; Wang, R.; Zhuang, K.; Zhao, Y.; Wang, H.; Ali, M.A.; Xu, H.; Man, C. Gold nanoparticle-based enhanced lateral flow immunoassay for detection of *Cronobacter sakazakii* in powdered infant formula. *J. Dairy Sci.* **2018**, *101*, 3835–3843. [[CrossRef](#)]
21. Kim, H.-S.; Ko, H.; Kang, M.-J.; Pyun, J.-C. Highly sensitive rapid test with chemiluminescent signal bands. *BioChip J.* **2010**, *4*, 155–160. [[CrossRef](#)]
22. Park, S.; Kim, H.; Paek, S.H.; Hong, J.W.; Kim, Y.K. Enzyme-linked immuno-strip biosensor to detect *Escherichia coli* O157:H7. *Ultramicroscopy* **2008**, *108*, 1348–1351. [[CrossRef](#)]
23. Shin, J.H.; Park, J.K. Functional Packaging of Lateral Flow Strip Allows Simple Delivery of Multiple Reagents for Multistep Assays. *Anal. Chem.* **2016**, *88*, 10374–10378. [[CrossRef](#)] [[PubMed](#)]

Disclaimer/Publisher’s Note: The statements, opinions and data contained in all publications are solely those of the individual author(s) and contributor(s) and not of MDPI and/or the editor(s). MDPI and/or the editor(s) disclaim responsibility for any injury to people or property resulting from any ideas, methods, instructions or products referred to in the content.